Quantify large population following climate disasters using satellite remote sensing imagery

Aness Chelfat (aness@aims.ac.za)
African Institute for Mathematical Sciences (AIMS)

Supervised by: Dr. Houriiyah Tegally
Co-Supervised by: Dr. Moritz Kraemer
Stellenbosch/Oxford , SA/UK

16 June 2024

Submitted in partial fulfillment of a structured masters degree at AIMS South Africa

Abstract

Disasters related to climate change increasingly lead to large-scale population displacements with social, economic, or environmental impacts. This study aims to quantify these movements using satellite remote sensing imagery; for this work, the African continent was the focus, where these events increased in frequency between 2000 and 2018. By analyzing high-resolution satellite images and integrating additional data sources like Landscan population counts, this research aims to link climate disasters with subsequent population movements. The methodology involves a comprehensive data collection process, merging datasets from the Emergency Events Database (EM-DAT) and the Global Disaster Information System (GDIS) with remote sensing data from sources such as Copernicus Climate Data and Dynamic World. This integration is made possible by using Google Earth Engine and its extensive data catalog and the Python library *Geemap*, enabling us to perform a detailed analysis of population distribution changes before and after disaster events. The study employs yearly and monthly analyses to find short-term and long-term human displacement trends. Geographic Information Systems (GIS) techniques and change detection models are used to evaluate land cover changes and validate observed population shifts. We also tried to use displacement data or Sentinel-2 imagery to validate these changes further. Our findings indicate that climate disasters in Africa have caused population displacements. The results show patterns indicating that people moved from areas affected by climate disasters to safer regions. This research fills significant gaps in our understanding of climate-induced migration, particularly in Africa. It enhances scientific knowledge and helps develop practical tools and strategies for managing climate-induced migration and its impacts.

Declaration

I, the undersigned, hereby declare that the work contained in this research project is my original work, and that any work done by others or by myself previously has been acknowledged and referenced accordingly.

Aness Chelfat, 6 June 2024

Contents

1. Introduction

Quantifying large population movements after climate disasters, such as floods, storms, and heat waves, using satellite remote sensing images is a field with great potential (Chen, 2020). Understanding this link between migration and climate hazards is essential to creating strategies for future mitigation. Proper measurement of these movements will help with effective disaster response, appropriate resource allocation, decision-making, and it could help inform enhanced modeling activities on the impacts of climate change on human migration.

Climate-related disasters typically involve short-term and long-term population displacements. Such movement can lead to significant social, economic, and environmental considerations. Remote sensing technology allows a thorough analysis of climate processes and patterns of human migration. Although some past studies have highlighted the potential of remote sensing in understanding human migration (Chen, 2020)], very few efforts, particularly in Africa, where climatic disasters are becoming even more frequent, have exploited this technique in tracking population displacement (Tellman et al., 2021).

Xu and Freitas (2009) finds that frequent and severe natural disasters, such as cyclones, floods, and riverbank erosion, lead to significant displacement and migration. Bangladesh's geographical location and socioeconomic conditions exacerbate the impacts of these disasters on human populations. Disaster-induced migration is often temporary, with people returning to their homes once conditions improve. However, repeated disasters can lead to permanent migration and changes in settlement patterns, contributing to urbanization and increased pressure on urban infrastructure. Wang et al. (2020) notes that shifts in climate conditions, such as increasing temperatures and changing precipitation patterns, can alter agricultural productivity, water availability, and habitability of regions. These changes often force communities to migrate in search of more favorable living conditions. Prolonged droughts or floods can devastate livelihoods, prompting both short-term and long-term migration. Migration can be a coping mechanism for environmental stress, but it also poses challenges for both sending and receiving areas.

1.1 Problem statement

All of us are aware that in the event of disasters related to climate change, most of the time, several people would be forced to evacuate their homes. This gives rise to question: How can one, with the use of remote-sensing images over the African continent, measure the movement of people after climate-related disasters?

1.2 Why is it important?

These movements must be measured for effective humanitarian responses, policy planning, environmental management, social integration, and research on climate change that could help inform enhanced modeling activities into the impacts of climate change on human migration. This way, we enhance the understanding of the impacts of climate disasters.

1.3 Objective

One of the study's objectives is to develop methodologies that can be applied to analyze population movements following climate disasters using remote sensing imagery. We want to come up with answers that improve our understanding of African displacement patterns and trends. This will lead to a more informed and effective responses to climate-related displacement.

To achieve these objectives, the study will adopt various methods. First, it will compare high-resolution satellite images taken before and after the disasters in Africa to identify possible changes in population distribution. In this case, multi-temporal satellite data, derived Land Use Land Cover data, and data related to climate disasters will be used for the analysis, and other data, such as the Land scan population count, would be integrated into the research to give an altogether human movement scenario with regard to climate disasters.

The main analysis will pursue the general relationship relating specific disaster-related events to resulting population movements, concentrating on short-term and long-term trends

1.4 Expected results

This research is crucial because it tackles some gaps in our understanding of climate-induced migration, mainly focusing on Africa, a continent frequently affected by climate events (Thomas and López, 2015). By using advanced remote sensing and combining data from multiple sources, this research aims to fill those gaps. Results will include information in dealing with disaster response and resource allocation. It would also be an improvement for the scientific knowledge and help in usable strategies for climate-induced migration.

2. Background

Climate-related disasters have been linked to extreme weather events that have risen due to changes experienced in the globe's climate (Thomas and López, 2015). They include many natural catastrophes that significantly affect populations and environments. Heavy precipitations lead to floods, in the process, destroy lives and infrastructure (Walls et al., 2023). Hurricanes. These are intense tropical cyclones with extremely active winds and rainfalls leading to large-scale destruction (Fang et al., 2020). Droughts These are comparatively long durations of significantly below-average precipitations leading to extreme shortages of water, crop failures, and adverse effects on many ecosystems. That is when it would lead to severe wildfires, and destroy homes, wildlife, and natural resources. Also, heatwaves can bring severe health emergencies which primarily affect older people, children, and people who have pre-existing sicknesses. Thus, it has been recognized increasingly today as one of the most significant factors that influence migration patterns (Mbaye and Okara, 2023; Ofori et al., 2023).

These impacts of environmental change can be directly or indirectly since the human population is affected. This has created an increasing international interest in measuring migration accurately (Hoffmann et al., 2020). Though the conventional approaches of collecting data through Census or Survey or administration could create a baseline understanding(Hugo, 2006; Bilsborrow et al., 1997). New technologies, and techniques now can capture the complex dynamics of climate-induced migration (Blumenstock, 2012b; Zagheni et al., 2014). Innovations like mobile phone data usage, social media data, and online search data have great potential to transform migration studies with real-time information on mobility in human beings.

2.1 Climate-Induced Migration: Causes, Patterns, and Consequences

Cyclones, floods, and erosion are frequent natural disasters and often of such severity that they cause substantial displacement. As it has already been introduced in the introduction, Xu and Freitas (2009) adds to this line of reasoning that the the geographical vulnerability of Bangladesh makes these impacts even stronger and causes permanent and temporary migration. What disaster does to an area is transform it into an uninhabitable place, thus creating instant evacuation and displacement possible. The disaster-induced migration is mostly temporary since migrants would go back home as soon as everything has returned to normal. However, repetitive disasters and or highly disastrous ones cause permanent migration. Xu and Freitas (2009) reminds us that this type of migration even induces urbanization since the displaced populations migrate to urban centers in search of employment and better living conditions.

It is because of changes in climate conditions due to continuous rise in temperatures and changing precipitation patterns that influence agricultural productivity levels and the available water levels (Wang et al., 2020), which eventually affect regional habitability and thus cause migration of the community to better living conditions, so the report argues. More extended drought or flood events destroy the agricultural livelihood, causes short-term displacement and a long migration period of the affected populations into favorable ecological settings.

2.1.1 Causes of Climate-Induced Migration

Natural disasters are instant causes of migration. These lead to the destruction of infrastructure, homes, and agricultural land, hence making people move. For example, tropical cyclones have been known to cause massive displacement due to the destruction of housing and infrastructure (Fang, 2020).

The gradual changes in rising temperatures, sea-level rise, and altered precipitation patterns affect the productivity of agriculture and, hence, water availability.

These changes can make their areas less livable over time, providing a reason for migration as a long-term adaptation strategy, among others (Wang et al., 2020).

2.1.2 Patterns of Migration

Migration can be temporary or permanent. Temporary migration occurs in case the individuals or families leave their homes for a short period. Permanent migration happens in case people move permanently because of persistent adverse conditions or repeated natural disasters (Xu and Freitas, 2009). In most cases, the displaced populations are usually shifted from rural to urban areas. Urban areas have better job opportunities and good standards of living. A process like rural-urban migration may cause urbanization, thereby putting pressure on the urban infrastructural setup and services (Hoffmann et al., 2020).

2.1.3 Implication of Climate-Induced Migration

There could be rapid urbanization whereby cities and industries grow because of increased migration to urban centers. It would also pressure urban resources, infrastructure, and services, besides the requirement of superior and more efficient urban planning and policies to entertain a more significant population within the region (Hoffmann et al., 2020). Migration may have a positive or negative influence on the country's economy. It will ease some of the strains on over-exploited rural environments. However, it can also work to create shortages of workers in rural locations and heighten competition for employment opportunities within urban centers (Wang et al., 2020). Inadequate housing conditions, restricted access to healthcare services, and issues of social integration are some of the problems migrants often face. These challenges prove further that there is a need for all-encompassing policies that guide migrants on maintaining or improving their well-being in new environments (Health, 2020).

2.2 Related work

This study by (Bernzen et al., 2019) was intended to determine the causes of migration in the rural households residing along the coastlines of Bangladesh, which have dramatically been impacted by climate change. This paper uses remote sensing data to examine environmental stress factors, including severe river erosion and proximity to major waterways and determined that a small percentage of the people residing along the rural coasts migrated mainly temporarily and domestically. These reasons ranged from better employment opportunities, marriage, family reunification, and education. It points out, though, that economic factors are the main drivers, with environmental stressors playing a significant role in decisions taken by migrants.

Joyce et al. (2009) point out that satellite imagery has become very relevant in emergency mapping and monitoring. Zagheni et al. (2014) explains how, for situational awareness and decision-making purposes on disasters, satellite imagery can offer high resolution in real-time, which helps the coordination among relief agencies. Zagheni et al. (2014) also presents the use of Earth Observation (EO) sensing for internally displaced people camp monitoring and population dynamics in conflict areas. The changes to the camps are monitored using EO data, and this guides humanitarian response on population distribution as well as the living conditions in such camps.

Yet, both of these studies reveal a need for integration with other sources of information and require more skill in advanced interpretation of imagery. This includes problems with the accessibility of data and ground validation.

Karantanellis et al. (2023) uses satellite imagery to map liquefaction phenomena caused by the Türkiye-Syria earthquakes. Satellite data rapidly picked out signs of earthquake-induced ground deformations. In this sense, it can help disaster response and infrastructure planning. An apparent strength is that satellite data rapidly covers large areas. A weakness may be the often high resolution needed in the image data and its cost, in addition to demands on data processing.

In this perspective, Silva-Coira et al. (2020) evaluates erosion and accretion along the Ganges River. To this end, the study was undertaken by applying remote sensing and GIS techniques to bring out a far more detailed analysis of the spatial and temporal changes that are compulsory for flood hazard management and sustainable development. Singh et al. (2023) is praised for being methodology-oriented but should be strengthened by community-based observations that validate remotely sensed data. Health (2020) discusses health impacts resulting from climate-induced migration. Rising cases of malnutrition, infectious diseases, and mental disorders, among other related health problems, tend to escalate due to such artificial changes in climatic phenomena. It also pleads for an integrated health and migration policy framework to address such issues. However, the paper can explore further into long-term health implications, as well as healthcare infrastructure, in an account of migrant health.

3. Methods

3.1 Introduction

The increasing frequency of climate disaster events, such as floods, storms, droughts, and heatwaves, have impacts on populations (Chen, 2020), often resulting in both short-term and long-term movements. This chapter aims to explore the application of remote sensing technology to provide a detailed analysis linking climate events with human displacement. This chapter outlines the methodology used to integrate remote sensing data with human movement patterns, the analytical techniques employed, and the case studies examined. Through this approach, looking to fill the gap in existing literature and provide valuable insights into the intersection of climate change and human mobility in Africa.

3.2 Data collection

3.2.1 Disasters Datasets

The Emergency Events Database (EM-DAT) (Centre for Research on the Epidemiology of Disasters (CRED), 2024) is a global database managed by the Centre for Research on the Epidemiology of Disasters (CRED), it records the occurrence and effects of over 26,000 natural and man-made disasters from 1900 to the present. EM-DAT compiles data from a variety of sources to help in providing valuable insights into the health and economic impacts of disasters at a country level.

The database includes both quantitative and qualitative data describing the frequency, impact, and characteristics of disasters, it contains the type of disaster (e.g., floods, storms, heatwaves), the full date of occurrence, affected regions, and causalities. However, it lacks spatial information, as the majority of the 'Latitude' and 'Longitude' fields are incomplete.

The Global Disaster Information System (GDIS) (Rosvold and Buhaug, 2021a,b) provided by the United Nations Office for Disaster Risk Reduction (UNDRR), builds on the EM-DAT Database by adding GIS polygons. This enhancement fills in missing 'Latitude' and 'Longitude' details, providing more precise location data for disasters.

3.2.2 Remote sensing data

Using Landscan global data (Bright et al., 2008, 2010), which is a premier population distribution dataset developed by Oak Ridge National Laboratory. It provides high-resolution global population data, which is crucial for various applications, including emergency response, disaster management, and risk assessment. The dataset uses advanced spatial data and imagery analysis to estimate population distribution across a 1 km^2 grid, updated annually to reflect changes and trends.

Using the Copernicus Climate Data (Liu et al., 2023), which provides detailed information on the Earth's surface composition. This dataset is essential for our studies, It includes annual global land cover maps at a 300-meter resolution derived from satellite imagery, offering high-resolution data that covers 22 distinct land cover types such as urban areas, croplands, and forests.

Using Dynamic world data (Brown et al., 2022) , which is a global land cover mapping tool created by Google Earth Engine and World Resources Institute. It provides high-resolution, near real-time data on land cover changes at a 10-meter resolution. It uses AI and satellite imagery to offer detailed insights into various land cover types, including forests, urban areas, and water bodies.

By examining changes in land cover over time, we aimed to identify areas experiencing rapid urbanization, deforestation, or other alterations that may contribute to displacement and migration.

3.2.3 Validation data

The Global Flood Database, Tellman et al. (2021) provides information about global flood events. It provides details of the extent, duration, and frequency of floods. It efficiently monitors and manages floods by giving easily accessible, understandable, and complete data on floods obtained from satellite imagery. More than 15 years of flood data are available for various use cases linked to disaster response, risk analysis, and climate change adaptation.

The data for all internal displacement is held in the IDMC Global Internal Displacement Database-GIDD (, IDMC). This provides an analysis of displacement caused by, in our case, natural disasters; data from 2008 to 2023 is available. The interface allows users to explore, filter, and visualize the data and download it in multiple formats.

3.3 Data analysis

3.3.1 Cleaning the disaster data

Before analysis, it is crucial to conduct data cleaning separately for the EM-DAT and GDIS disaster datasets to ensure consistency and readiness for analysis.

For the EM-DAT dataset, we began by removing any missing values from the EM-DAT dataset to maintain data integrity. We then extracted the relevant columns: 'disasterno', 'Country', 'Location', 'Disaster type', 'Year', 'Date', and 'Total deaths'. Next, we unpacked the locations from a list of locations into individual entries. To ensure consistency, we aligned the disaster numbers by removing any extra characters. Finally, we filtered the records to include only disasters that occurred between the years 2000 and 2018.

Disasterno	Country	Location	Disaster type	Year	Date	Total deaths
1999-9388	Djibouti	Ali Sabieh	Drought	2001	2001-06-01	0.0
1999-9388	Djibouti	Dikhil	Drought	2001	2001-06-01	0.0
1999-9388	Djibouti	Djibouti	Drought	2001	2001-06-01	0.0
1999-9388	Djibouti	Obock	Drought	2001	2001-06-01	0.0
1999-9388	Djibouti	Tadjourah provinces	Drought	2001	2001-06-01	0.0

Table 3.1: Example of EM-DAT dataset after cleaning (Centre for Research on the Epidemiology of Disasters (CRED), 2024)

For the GDIS dataset, we cleaned the data by selecting the relevant columns: 'disasterno', 'Country', 'Location', 'Disaster type', 'Year', 'Latitude', and 'Longitude'. After this, we filtered the records to include only disasters that occurred between the years 2000 and 2018.

Disasterno	Country	Location	Disaster type	Year	Latitude	Longitude
4029	Burundi	Vugizo	Flood	2018	-4.153846	29.678495
4030	Burundi	Gatumba	Flood	2018	-3.312979	29.242054
4031	Algeria	El-Bayadh	Flood	2018	32.565401	0.911589
4032	Algeria	Tiaret	Flood	2018	34.965109	1.530424
4033	South Sudan	Unity	Drought	2009	8.926421	29.885783

Table 3.2: Example of GDIS dataset after cleaning (Rosvold and Buhaug, 2021a,b)

While the EM-DAT dataset provides precise date information, it lacks detailed spatial data. On the other hand, the GDIS dataset contains coordinates for more accurate location information. By merging both datasets using the common fields 'disasterno', 'Location', 'Country', 'Disaster type', and 'Year', a more comprehensive dataset was created. This final dataset that contains '43374' rows is enriched with both spatial and temporal information, providing a more accurate analysis.

Disaster No.	Country	Location	Disaster Type	Year	Date	Total Deaths	Latitude	Longitude
2018-0162	Algeria	Tiaret	Flood	2018	2018-04-24	6.0	34.965109	1.530424
2018-0232	Niger	Maradi	Flood	2018	2018-06-01	36.0	14.116153	7.299178
2018-0292	Sudan	West Kordofan	Flood	2018	2018-07-23	23.0	11.761982	28.405309
2018-0365	Nigeria	Kogi	Flood	2018	2018-09-20	199.0	7.716356	6.696042
2018-0387	Sudan	Kassala	Flood	2018	2018-08-01	23.0	15.988691	35.750775

Table 3.3: Combination of EM-DAT and GDSI data (Rosvold and Buhaug, 2021b)

After cleaning the data, we saved it as a CSV file and used *Geemap* to create feature collections that contained spatial information in the form of 'country', 'date', and 'coordinates' for each disaster. We then added layers for each disaster type, assigning a unique color to each type (e.g., Flood: 'Half Baked', Storm: 'Lavender Gray', etc.), and created an Earth Engine map (Figure 1). This visual representation allowed for clear and effective analysis of the spatial distribution and impact of various disasters.

3.3.2 Analyzing remote sensing data

Using remote sensing imagery is crucial for identifying trends and patterns in human movement following climate disaster events. This analysis starts by using *Geemap* to read the Image collections provided by Google Earth Engine data catalog and crop it with Africa shapefile.

The calculation of population change involves a comparison of Image from the image collections for each year. This is done by subtracting the population of the future year from the population of the following year, which provides a clear measure of the change in population over time. Iterate over the disaster records, adding each disaster locations using their Latitude and Longitude to the map with a color corresponding to the disaster type (e.g., Flood is blue, Drought is yellow ..).

$$population \quad change(t) = population(t+1) - population(t-1) \qquad with \quad t : year$$

Now, we can extract the population movement after a disaster by clipping to two areas of interest, one is affected by the disaster and the other one is where we notice increase in urban and population count by looking at the map. we defined a point with specified coordinates and created a buffer around this point. We took this buffer to quantify population increase and decrease. This approach allows us to quantify the population dynamics after the disaster. For example, in a city, we can define a buffer covering the city and measure the population count—in or out—of the town.

Population change data is then integrated with land cover change data from the Copernicus Climate Data (Gorelick et al., 2017) with 22 different classes. This spatial and temporal information allows for a comprehensive analysis of the relationship between population changes and land cover changes. For example, to understand the impact of disasters in the year 2008, we examine the changes in population and land cover between the years 2007 and 2009, and the change is done the same as the population change, meaning subtracting the land cover of the future year from the land cover of the previous year. Finally, we validate the data by confirming the people displacement using IDMC data (, IDMC). By analyzing the data from the year before and the year after each disaster, we can better understand the impacts of climate disasters on human settlements and environmental conditions. Additionally, this approach helps us understand urban change, showing the increase of urban areas and population in some areas.

Once these general trends are established, the analysis moves to a more detailed level. We filtered the disaster data from June 27, 2015, to December 31, 2018, due to the availability of Dynamic World data. By focusing on this period, we can leverage the high-resolution, near-real-time land cover information provided by Dynamic World. This approach allows for detailed observation of migration patterns and land cover changes within the affected areas.

We explored the time series of each class to understand the temporal patterns, we chose randomly an area that is affected by climate disaster, We filter the Dynamic World collection to include images captured over this location within the desired time frame, typically a year. This filtered dataset includes all class probability bands. We employed the *reduceRegion* method to compute mean values within the affected region at a scale of 10 units. We then mapped over the Dynamic World time series collection, generating a dataset of time-stamped mean band values for further analysis. Next, we converted the extracted time-series data into a structured format by transforming it into a DataFrame using Python's *Pandas* library. This tabular representation facilitated efficient data manipulation and analysis, with each row corresponding to a specific date and columns representing the band names alongside their respective mean values. To address any missing values in the dataset, we performed linear interpolation, ensuring continuity in the plotted time series. This allows one to build change detection models easily without training custom models or collecting training data.

Finally, we visualized the time series of class probabilities using *matplotlib*, a *Python* plotting library. Each band's class probabilities were plotted against time, with the x-axis representing dates and the y-axis indicating the probability values. To enhance readability, we included axis labels, a title, and a legend specifying the color-coded bands. This comprehensive approach enabled us to gain insights into the temporal patterns of land cover changes, contributing to a deeper understanding of environmental dynamics and informing our research on migration and climate disasters.

After this we built a change detection model using probability band, for each disaster event, we took the mean values of land cover data (dynamic world) as shown in Figure 3.1 for several months before and after the disaster, we didn't specify the number of months due to the lack of data caused by cloud cover in the satellite images, even though the data was cloud-filtered to some extent. Using the mean allowed us to handle data gaps effectively. For example, during a storm, there would be a lot of cloud cover resulting in missing data. By averaging the data, we ensure that the dataset is less influenced by short-term anomalies and more reflective of the general land cover conditions. (Google Earth Engine, 2024a) The mean helps to smooth out these shifts, providing a more stable and reliable dataset for analysis. This approach ensures a comprehensive and balanced view of the land cover over time, allowing for accurate assessment of the impact of disasters on land cover changes. By using the mean, we ensure that the dataset is less influenced by short-term anomalies and more reflective of the general land cover conditions, leading to more reliable and meaningful analysis of the impact of disasters.

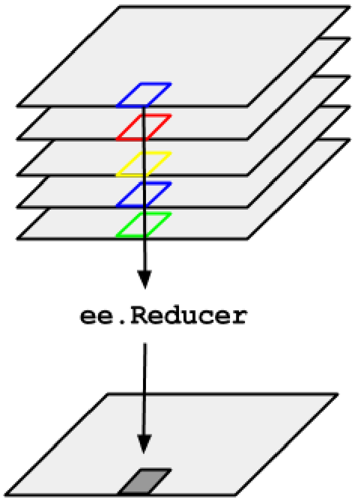

Figure 3.1: Reducer: average collection of images into a single image Google Earth Engine (2024a)

To find new areas for all eight land cover classes, we calculate the pixels that changed from an average probability below 0.2 to above 0.5. This method shows significant changes between the two images, such as transformations in urban areas, vegetation, water bodies, and other classes. For example, identifying new urban areas involves finding all pixels that had an average probability below 0.2 and then shifted to an average probability above 0.5.

$$new\ area = before\ disaster.lt(0.2).And(after\ disaster.gt(0.5))$$

Once these changes are identified, we generate an image where pixel values represent the area of each pixel using the predefined Google Earth Engine (GEE) function pixelArea(). This image is then multiplied by the new area binary mask (where 1 indicates change and 0 indicates no change), converting the binary mask into an image where each pixel value represents the area in square meters if there is a change, or 0 if there is no change.

Next, we sum the pixel areas within geometry using the *reduceRegion* function. This function reduces the region to a single statistic by specifying parameters such as the reduction operation (*ee.Reducer.sum()*), the geometry, the scale (10-meter resolution if the area is small and 1000 meter resolution if the area is too big), *maxPixels* set to 1e9 (the maximum number of pixels to process), and *bestEffort* set to True to ensure the function completes the calculation within computational limits. The result is a feature collection where the key is the band name and the value is the sum of the areas in square meters for a single feature.

This process allows us to accurately measure the area of land cover changes across all eight classes, providing valuable insights into urban development, vegetation changes, water body dynamics, and other significant land cover transformations. By using the mean, we handle data gaps effectively, such as those caused by cloud cover during storms, ensuring that the dataset is less influenced by short-term anomalies and more reflective of the general land cover conditions. This comprehensive and balanced approach allows for accurate assessment of the impact of disasters on land cover changes.

To validate the observed changes, we used high-resolution satellite data from Sentinel-2, which provides optical imagery at resolutions of 10, 20, and 60 meters, allowing for detailed environmental monitoring and land cover analysis (ESA Sentinel-2). By comparing images from before and after the disasters, we could see changes in specific areas, indicating shifts in land cover and urban development. Additionally, we used the Global Flood Database to validate the displacement of people due to climate disasters, which provided data on the number of people displaced after each disaster (Tellman et al., 2021). This combination of high-resolution imagery and displacement data allowed for a comprehensive assessment of the impact of disasters on both land cover and human populations.

4. Results

4.1 Climate disasters

Figure 4.1 shows floods frequency in both EM-DAT and GDIS datasets from 2000 to 2018 in Africa.

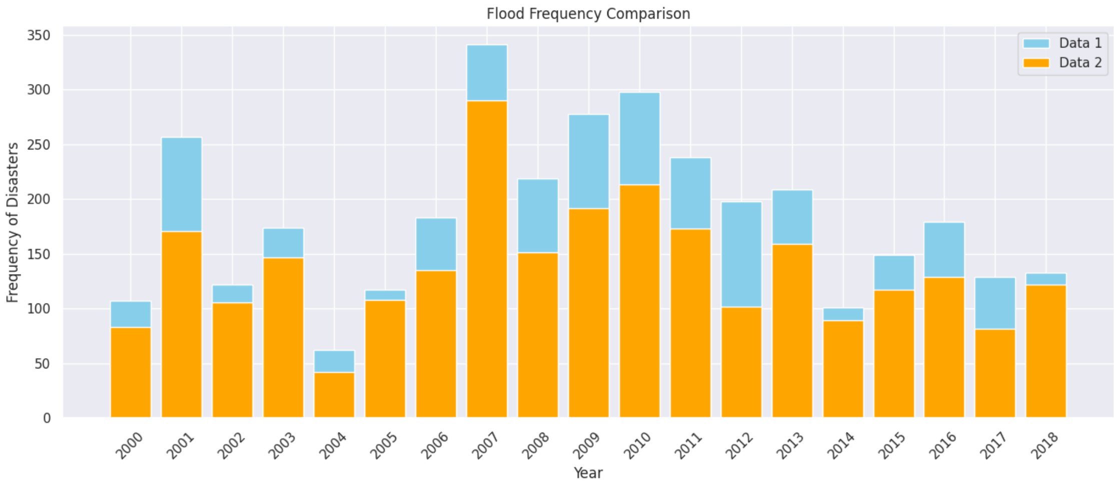

Figure 4.1: Flood frequency comparison between EM-DAT dataset and GDIS dataset from year 2000 to 2018 (Rosvold and Buhaug, 2021a,b)

Between 2000 and 2018, over 796 disasters, with floods (Figure 4.2) dominating the disaster count, accounting for 67% of the total. Storms (Figure 4.3) and droughts each comprised approximately 15% of the disasters.

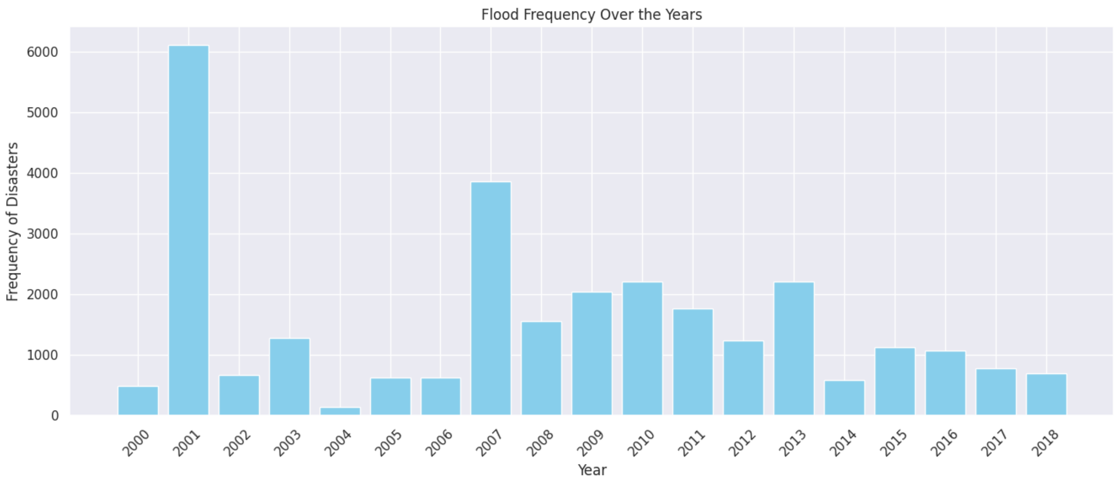

Figure 4.2: Flood frequency over the years between 2000 & 2018

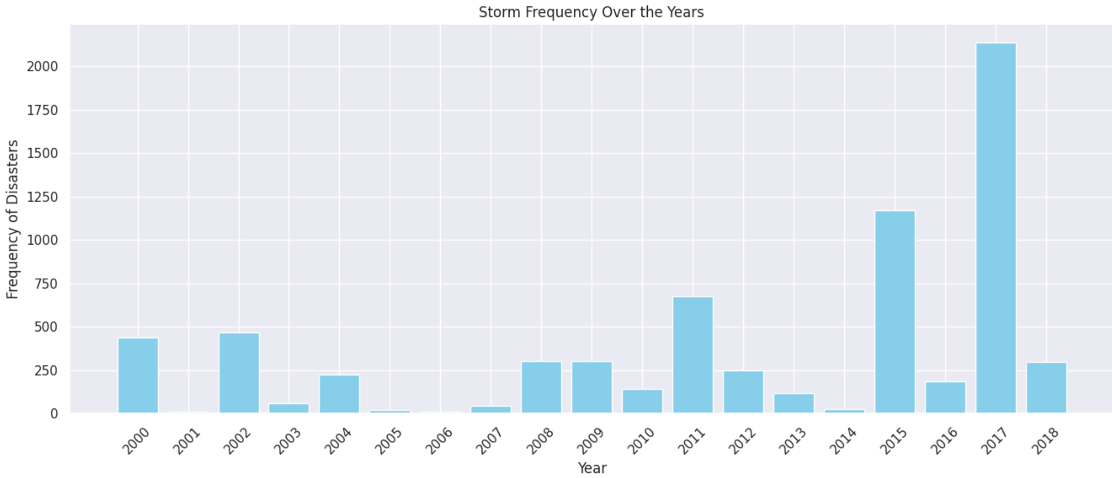

Figure 4.3: Storms frequency over the years between 2000 & 2018

From January 1, 2000, to June 26, 2015, there were 36,336 climate hazards. During this period, floods made up 71.34% of the disasters, droughts accounted for 15.34%, and storms constituted 11.56%.

In the nearly three years from June 27, 2015, to December 31, 2018, there were over 7,000 climate hazards. In this period, the distribution of disasters shifted significantly: floods decreased to 46%, storms increased to 38.14%, and droughts remained relatively stable at 15.78%.

- **Floods**: The percentage of floods decreased from 71.34% to 46.03%.
- **Storms**: The percentage of storms increased dramatically from 11.56% to 38.14%.
- **Droughts**: The percentage of droughts slightly increased from 15.34% to 15.78%.

This significant increase in the percentage of storms can be linked to climate change, which is known to influence the intensity and frequency of storms, including hurricanes and typhoons (Knutson et al., 2010). Droughts remain a consistent threat, with climate change potentially leading to longer and more severe droughts due to altered precipitation patterns (**?**). These trends highlight the growing impact of climate change on the frequency and distribution of weather-related disasters.

By plotting the spatial information using the python library *geemap*, we can gain more insight into the climate disaster dataset (Figure 4.4). For example, countries like Algeria, Kenya, and Mozambique have experienced a high number of disasters. Similarly, countries such as Madagascar, Uganda, Nigeria, Niger, Malawi, Angola, Ethiopia, and Sudan also show a significant number of disasters. However, the rest of the countries in West and Central Africa, as well as some parts of East Africa, have relatively lower numbers of disasters.

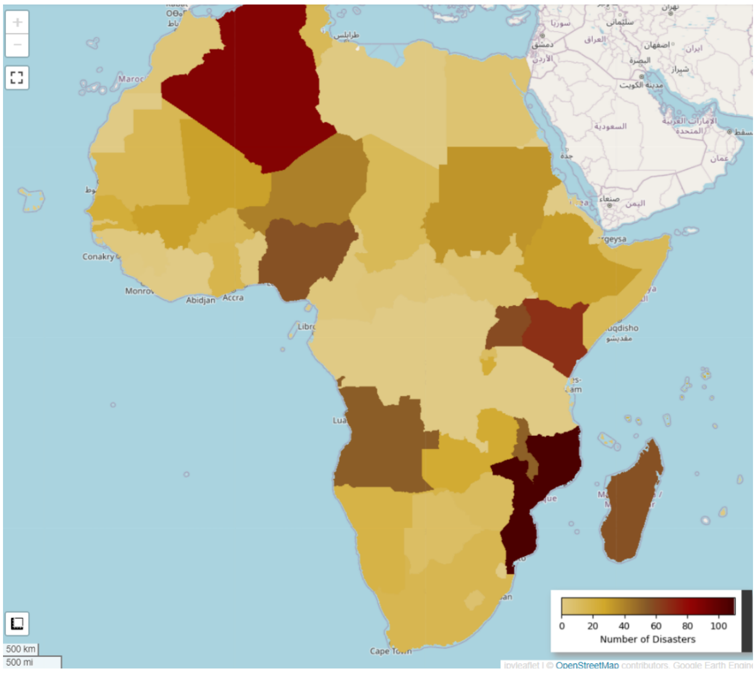

Figure 4.4: Disasters count in Africa between 2000 & 2018

Somalia has the highest number of deaths (Figure 4.5) caused by climate disasters on the continent, ranging from 15,000 to 20,000. Algeria also has a noticeable number of deaths. In contrast, the remaining African countries report lower numbers of deaths, with many having very few or zero fatalities.

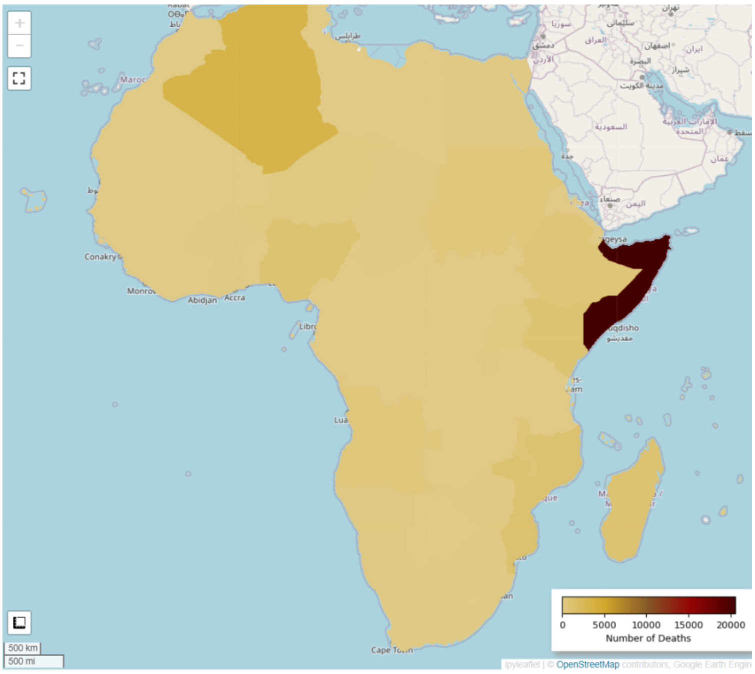

Figure 4.5: Deaths count in Africa between 2000 & 2018

Figure 4.6 is a geographical representation of the climate-related disasters that happened on the African continent between 2000 and 2018. It shows the entire African continent. The disasters are also distinguished as various types and colored accordingly: Floods - blue, Storms - yellow, Droughts- light blue, Earthquakes- green, Volcanic activity- red, and Mass movements (dry)- gray.

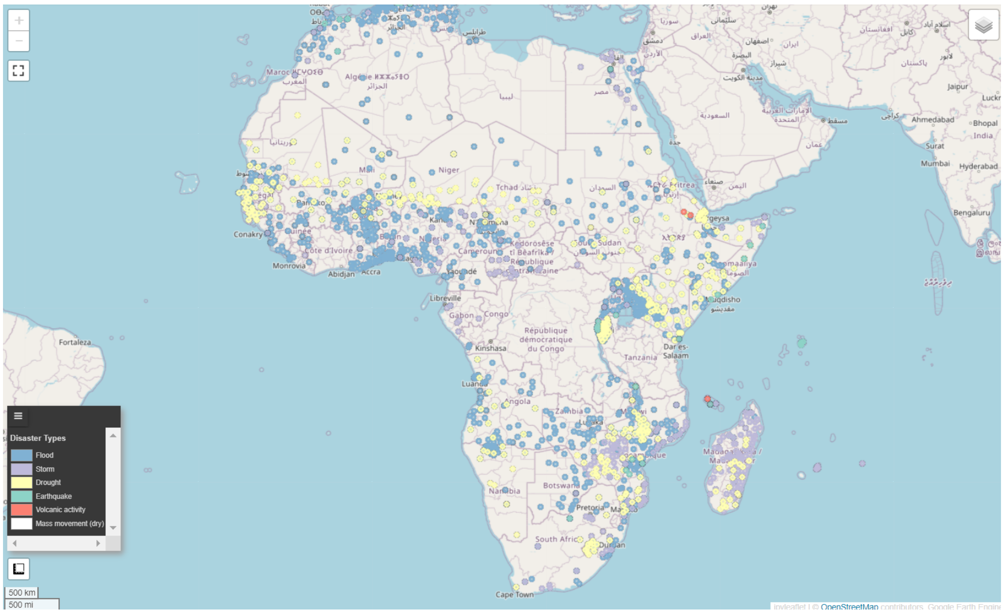

Figure 4.6: Climate disasters in Africa between 2000 and 2018 Centre for Research on the Epidemiology of Disasters (CRED) (2024); Rosvold and Buhaug (2021a,b)

We need only disasters from 2015 - 2018 for the monthly analysis due to lack of old data from dynamic world.

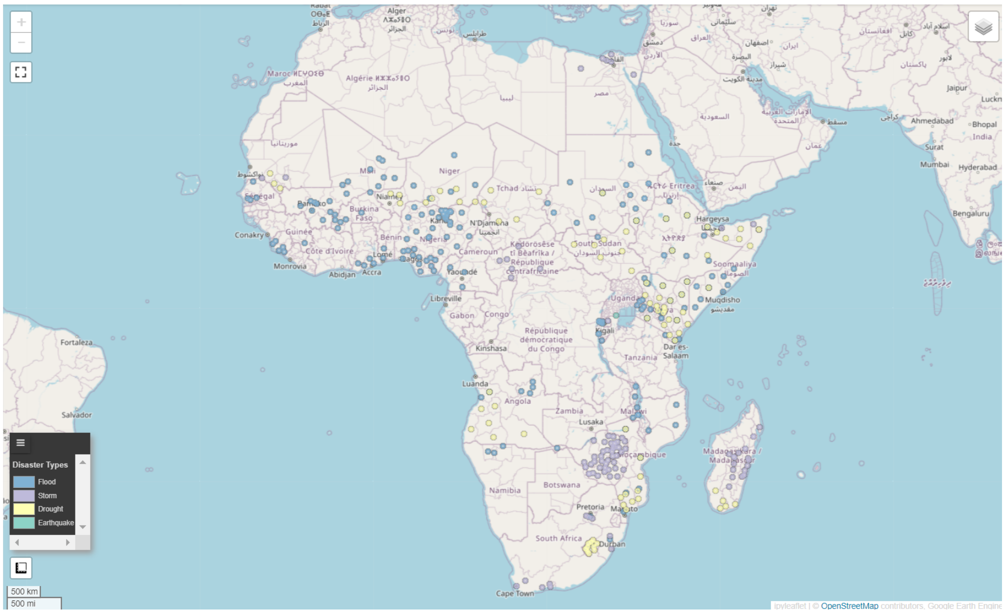

Figure 4.7: Disaster from 2015 to 2018 in Africa Centre for Research on the Epidemiology of Disasters (CRED) (2024); Rosvold and Buhaug (2021a,b)

The population in Africa shows a steady upward trend over the years (Figure 4.8), indicating consistent growth. In 2000, the population was slightly below 0.9 billion, and by 2018, it had increased to approximately 1.3 billion. The growth rate appears to be relatively consistent, with the population increasing steadily each year. There are notable increments between certain years, such as from 2004 to 2005 and from 2017 to 2018, where the slope of the line indicates a sharper increase in population. Overall, from 2000 to 2018, the population in Africa grew by about 0.4 billion people.

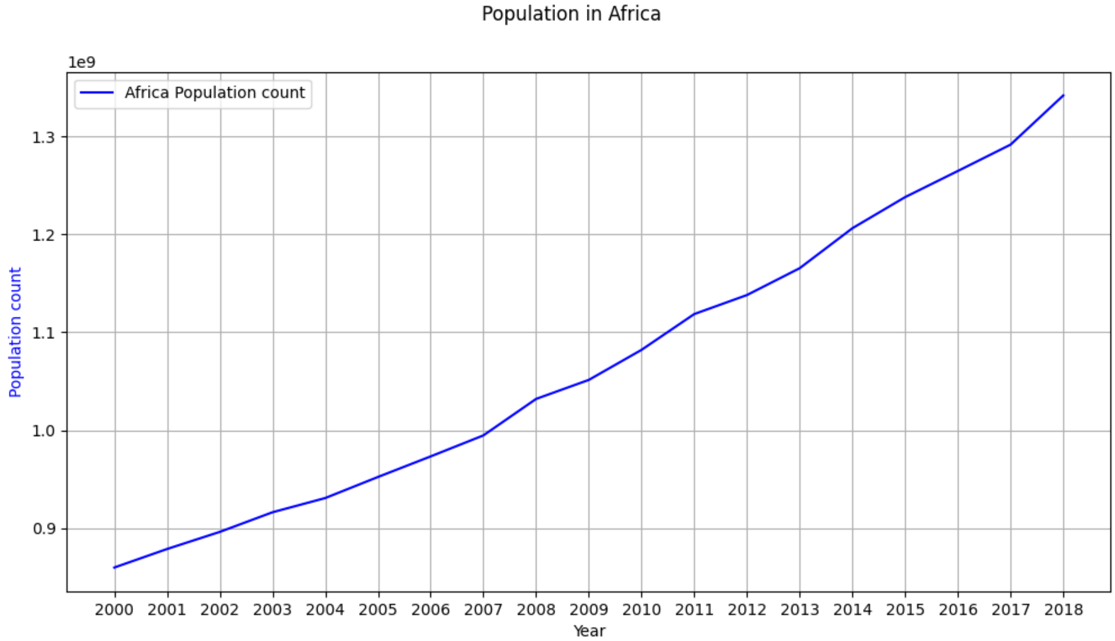

Figure 4.8: Population evolution in Africa over the years

The map in Figure 4.9 shows a varied spatial distribution of population changes, with some regions experiencing increases while others experience decreases. This variability could be attributed to multiple factors, including the impact of the disasters represented on the map.

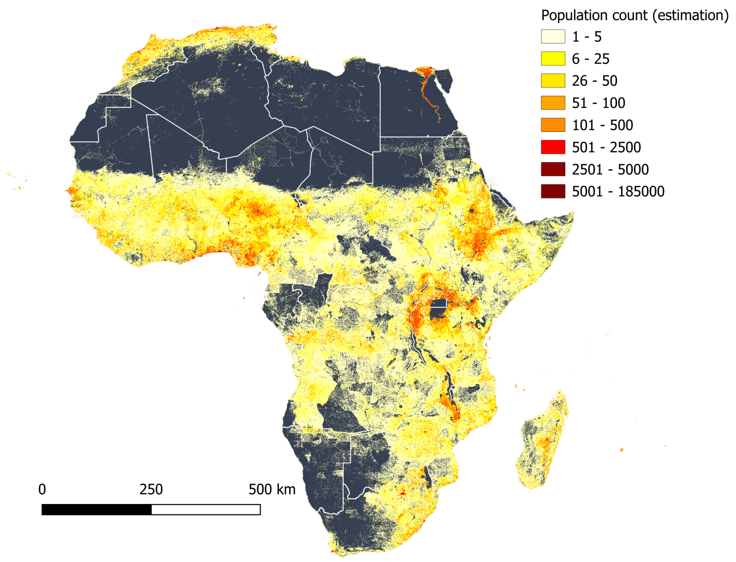

Figure 4.9: Population count (estimation) in Africa 2007 Bright et al. (2008)

4.2 Yearly Analysis of Population and Land Cover Changes related to climate disasters in Africa

We are going to Analyse each country individually. Although we have more than 20 countries affected by climate disasters over the years, we are going to include a few study cases chosen based on the severity of the people displaced, from the highest to the lowest. Using *Geemap* we will perform a change detection on both population and land cover data and try to link the climate disasters with people moving from the affected area to more safer region.

4.2.1 Study case 1: Niger 2011

Urban areas are dynamic, often experiencing significant transformations due to factors such as migration and environmental challenges. By monitoring these changes, we can gain insights for example into population movements. So we are going to perform change detection in urban areas and compare it with the change in population to check population movement.

In the Figure 4.10, we observe the urban changes and population shifts within the capital of Niger. The map on the left highlights urban changes where green squares indicate an increase in urban areas, suggesting that new buildings have been constructed. This urban expansion could be due to migration into the area or a response to the need for more secure housing solutions post-flood. Red squares represent a decrease in urban areas, likely because existing structures have been abandoned or damaged beyond repair due to the flood, prompting evacuations or relocations.

The map on the right displays population changes where green squares indicate an increase in population, suggesting that people have moved to these areas, likely seeking safer and higher ground or better living conditions after the flood. Red squares represent a decrease in population, likely because these areas suffered severe flood damage, making them uninhabitable and forcing residents to evacuate or move to other locations.

In Figure 4.11, we focus on the areas outside the capital. The left map shows urban changes, with green squares indicating some construction activity, but the extent is much less compared to the capital. Red squares represent a significant decrease in urban areas, likely because structures have been abandoned or destroyed by the flood, leading to a lack of reconstruction efforts. The right map displays population changes, with green squares indicating a minimal increase in population, localized compared to the capital. Red squares represent a notable decrease in population, suggesting that the flood damage outside the capital has been more severe or that these areas were less resilient, leading to a higher evacuation rate.

From Figure 4.10 and Figure 4.11, and after quantifying the population movement from these two areas after analyzing the changes. As shown in the Figure 4.12, about 56,380 people moved out of the left area and 14,9290 moved in, and around 568 people moved out to relocate to other location. we can see that despite the flood event, the population in the capital has shown resilience and even increased in certain areas. This suggests effective response measures and possibly people seeking better opportunities or safer locations within the city. On the other hand, areas outside the capital have experienced a decrease in population, indicating that the flood's impact was more devastating in these regions, leading to higher rates of evacuation and abandonment. This contrast highlights the difference in urban resilience and recovery capabilities between the capital and the outlying areas.

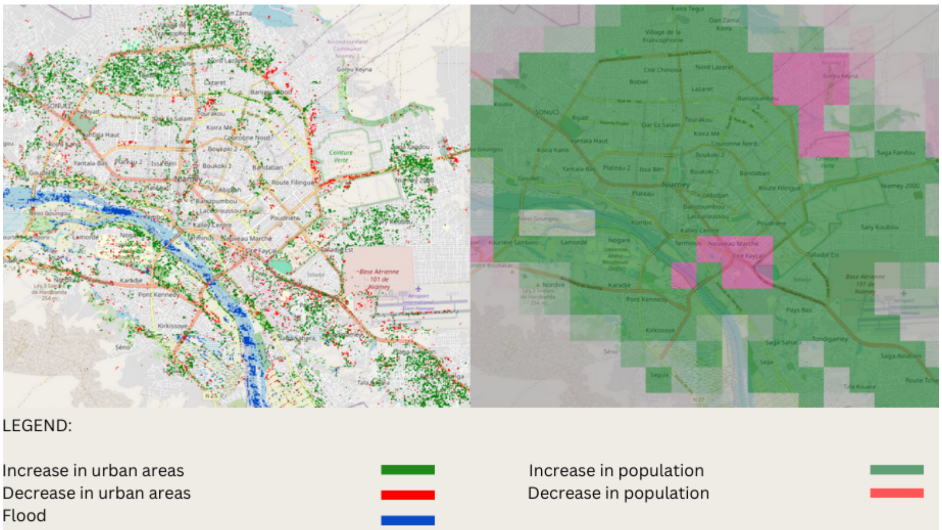

Figure 4.10: Change in urban areas and population in Niamey the capital of Niger(Liu et al., 2023)(Bright et al., 2008)

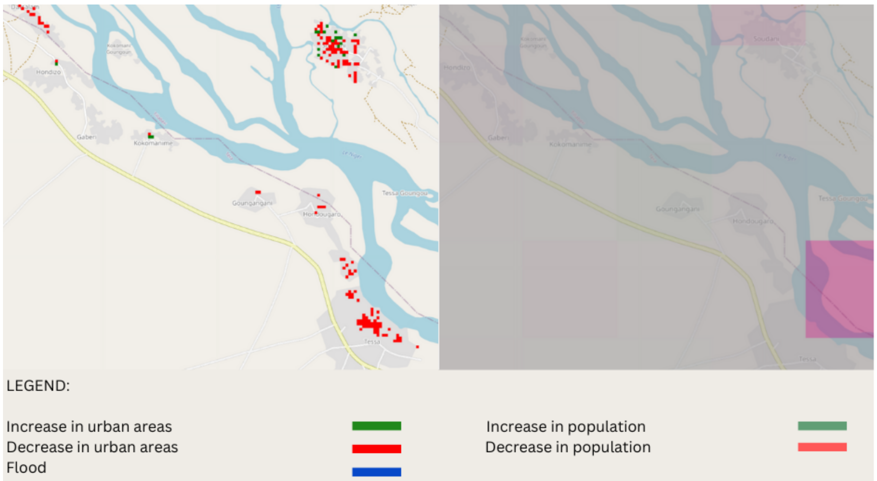

Figure 4.11: Change in urban areas and population outside the capital of Niger(Liu et al., 2023)(Bright et al., 2008)

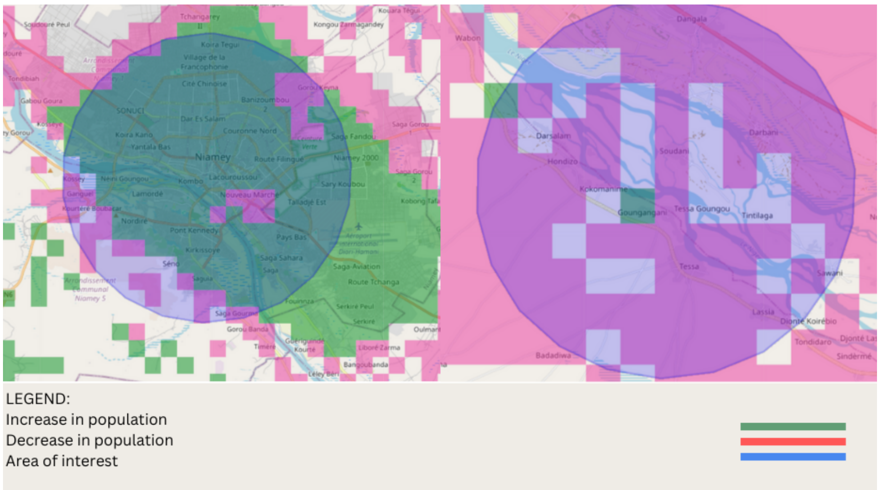

Figure 4.12: Change in population inside and outside the capital of Niger(Bright et al., 2008)

In addition to the map, data from the International Displacement Monitoring Centre (IDMC) gives an estimated 28,000 displacements due to the flood which occurred in Niger in 2011. While not all these displacements were from the area shown in the figure, it gives the local scale of the impact of the flood on the displacement of residents. The image, therefore, corresponds with the data that the IDMC has given out, showing that there was a massive movement of the population because of the flood.

4.2.2 Study case 2: Mali 2007

Figure 4.13 shows the changes before and after the disaster in urban areas and the population in Goundam Mali, specifically around the lac Oro. Different sections of the map are used to highlight various regions of interest. On the right is the population change before and after the disaster, and on the left is the change in urban areas.

The central map zooms in on the centre of the lake, Lac Oro, and the surrounding regions. Three areas of interest have been identified: 1, 2, and 3. Area 1 shows a decrease in urban areas, and population suggests that people have moved due to flooding. Areas 2 and 3 show increased urban areas and population count, indicating migration occurred from Area 1.

We measured the population movement by calculating the people that has moved-out of certain areas and the people that has moved-in in other areas. Figure 4.14 shows that approximately 5,073 moved-in to the areas on the right and 9,959 people moved out from the area near the river

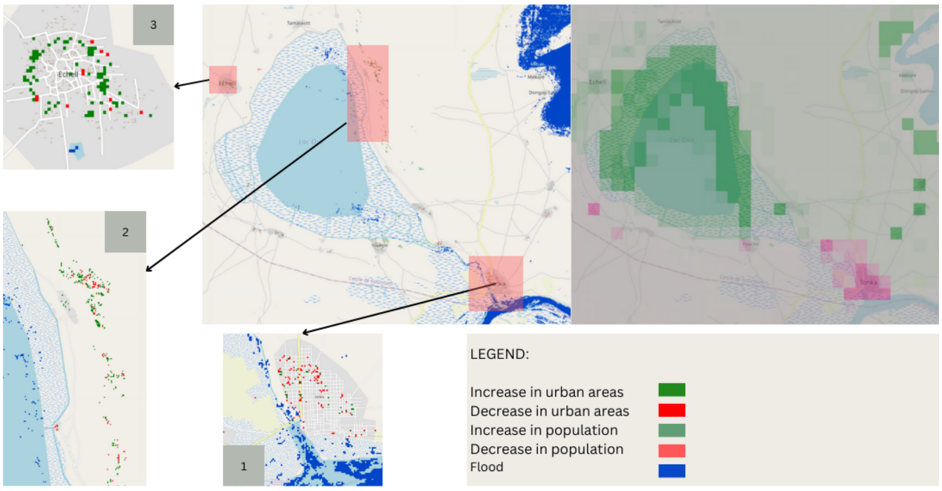

Figure 4.13: Change in urban areas and population in Goundam: Increase in both urban areas and population in some areas (2, 3) and decrease in other areas (1). suggesting that there was human migration.(Liu et al., 2023)(Bright et al., 2008)

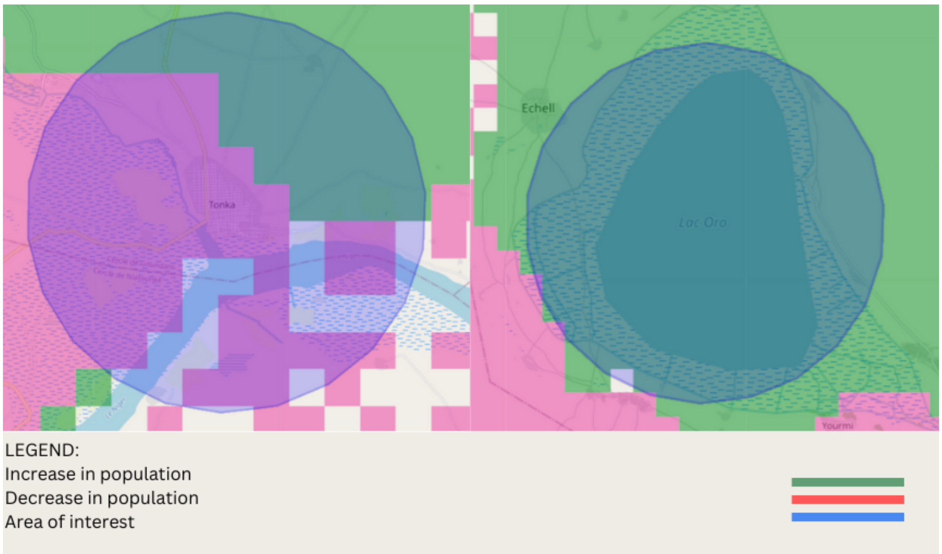

Figure 4.14: Change in population in Goundam (Bright et al., 2008)

Similar to Figure 4.13, Figure 4.15 shows that there was a decrease in both urban areas and population in areas near the river where the flooding occurred and an increase in other areas far from the river, indicate that people left their home due to flooding to new areas. Figure 4.16 shows a decrease in population.

As seen on the left side of the figure, it is estimated that roughly 2,885 people were displaced, and only about 91 persons moved-out.

We validated this to be the case: migration occurred in regions 2 and 3 and several regions around it. Using data from the Global Flood Database (Tellman et al., 2021), the number of people who migrate is approximately 540,000. The duration of the flooding was 76 days. Because of this large-scale flooding, the urban areas and population distribution experienced disruption, causing significant migration and change in these areas.

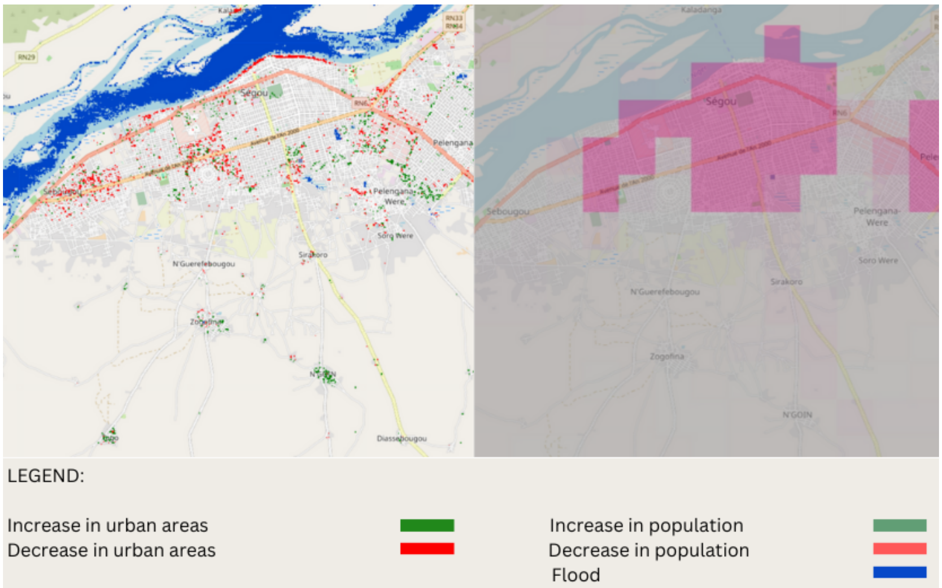

Figure 4.15: Change in urban areas and population in Segou: Increase in urban areas and population in some areas and decrease in others. Suggesting that there was human (Liu et al., 2023)(Bright et al., 2008)

Figure 4.16: Change in population in Segou (Bright et al., 2008)

In general, dynamic changes occur in urban development and population, where some areas expand at the cost of others. Those areas that show a decrease in population and an increase in urban areas indicate out-migration, probably due to flooding. Those areas that experience both population and urban area increases indicate in-migration.

4.2.3 Study case 3: Malawi 2015

The figure 4.17 shows changes in built-up areas and population before and after the disaster in different regions of Malawi, focusing on those parts that are located in the Chikwawa district. This figure 4.17 indicates changes in urban areas and population distribution where green squares represent increased urbanization and red represents decreased Built-up area. Light green color squares represent the increased population while light red color squares reduced the population. The flooded area is marked in blue color.

The bottom left part of the figure zooms on Dyeratu, showing in detail the urbanization changes, declines, and population shifts in this particular area. Next to it is Chobo, where there are changes in the urban areas, showing increased urbanization and an increase in population. This would indicate that some displaced populations from Dyeratu or other places have moved into Chobo.

We then quantified the population movement from these two areas after analyzing the changes. As shown in the Figure 4.18, about 1,034 people would move out of the left area, and around 364 people would move in to relocate to the right location. This analysis concludes that it would not be a case that the displaced population would move uniformly to the same location.

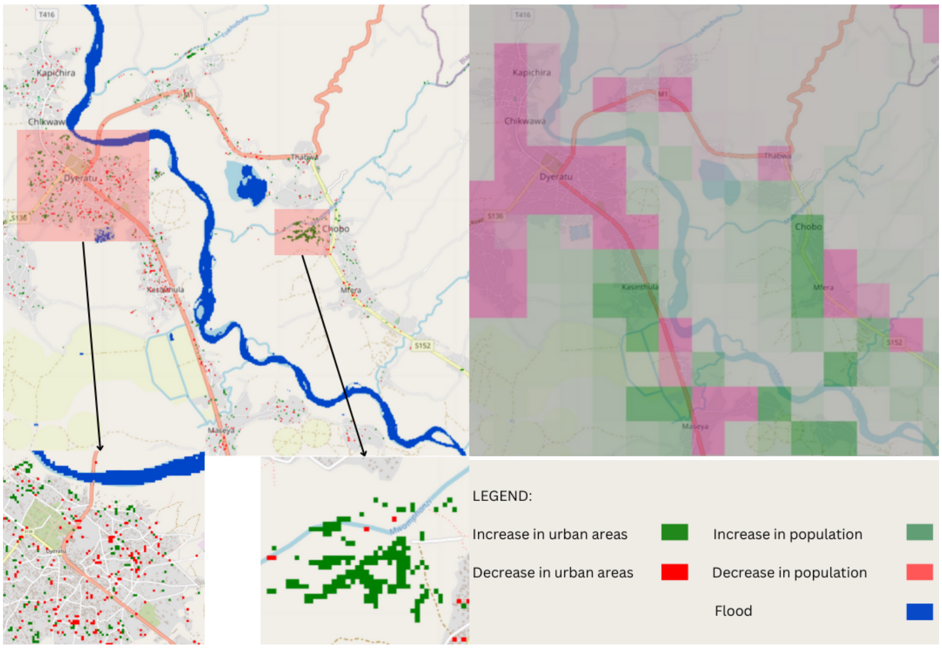

Figure 4.17: Change in urban areas and population in Chikwawa district in Malawi: Increase in both urban areas and population in some areas (2) and decrease in other areas (1). suggesting that there was human migration

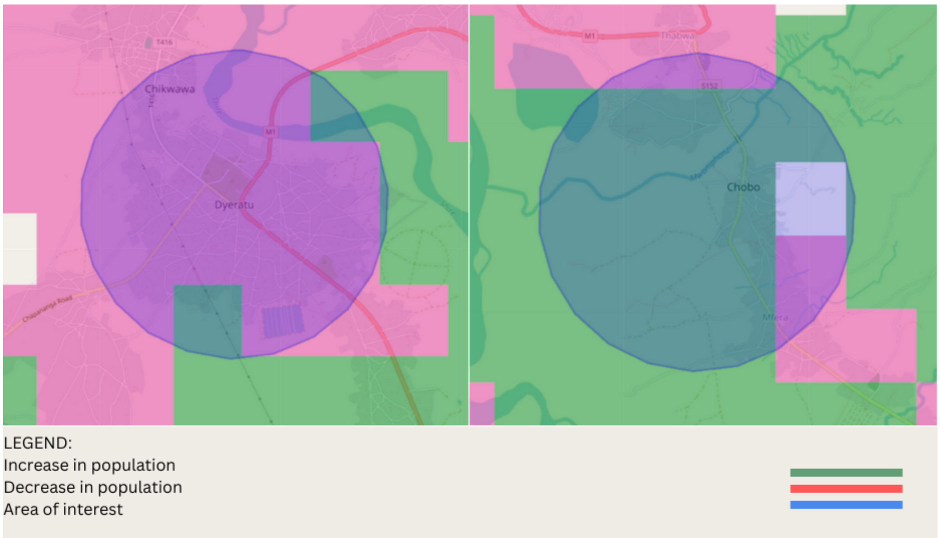

Figure 4.18: Population count (estimate) in the area of interest. (Bright et al., 2010)

4.3 Monthly Analysis of Population and Land Cover Changes related to climate disasters in Africa

After performing yearly analysis of population and Land cover changes related to climate disasters in Africa. In this section, we would like to have a more detailed and recent study based on data from Dynamic World. We will plot class probabilities. Change detection would later be performed using probability bands for further comprehension of disaster impact.

4.3.1 Study case 1: Ghana 2018

In Figure 4.19. On the left we shows a composite view of various land cover types across Ghana. Different colors represent different types of land cover. On the right, it focuses specifically on built-up areas extracted from the Dynamic World dataset. The built-up areas are highlighted in white, clearly showing urban and developed regions within the country.

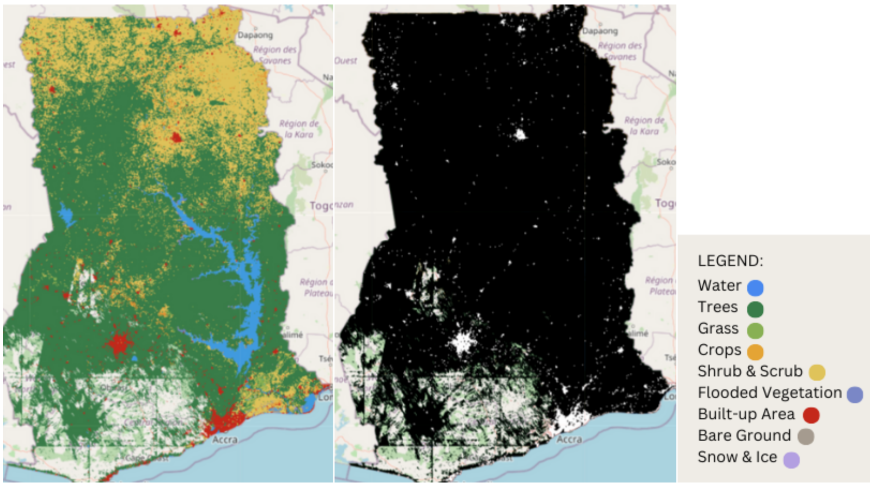

Figure 4.19: Dynamic World Composite and extracted built area image, Ghana 2018 (Brown et al., 2022)

Now, we are going to calculate the class probabilities over time for each class, to understand the temporal patterns.

The total number of pixels is 31,368, of which 155 pixels represent built areas, accounting for 0.49% of the total. The pixel distribution for different land cover types is as follows: there are 258 pixels for water, 2,739 pixels for trees, 124 pixels for grass, 21 pixels for flooded vegetation, 18,115 pixels for crops, 9,956 pixels for shrub and scrub, and 155 pixels for built areas.

Figure 4.20 is a visualization of the temporal change of the class probabilities. The different lines in the plot correspond to other land cover classes, which are distinguished by particular colors. The legend on the right-hand side of the plot identifies the land cover classes with their colors.

The "bare" class through the gray line and the "crops" class through the yellow line yield extreme peaks and troughs, hence large variability of their probabilities with time. We can learn how often changes in the areas classified as bare or as crops occur due to maybe seasonal agriculture activities, land management practices, and environmental factors driving soil exposure and crop growth.

From the category "water", peaks are on 27th August and 29 August,. It is showing that there is an increasing presence of water that causes events of rainfall, floods, or rivers to change course.

The class "built" shows peaks on 25 to 27, meaning that there were new areas that were classified as urban areas, and it matches with the date from the peaks in the water class, suggesting that there was a new built-up area or just a misclassification due to the clouds from the storm.

The pink line for the "snow and ice" class is relatively lower, more stable probabilities throughout the duration. It suggests that areas classified as built or snow and ice did not change much during this period. A lower probability for the class "snow and ice" may still suggest minimal cover with snow and ice, which indeed corresponds to a more significant part of the place and the season.

The class "grass" and the dark green line representing the class of "trees" produce an average variability. Peaks and probability change are present within the classes but not so carefully viewed as in the case of bare and crops. The changes in areas covered by grass and trees are taking place, but not that striking. Regular growth cycles, seasonal changes, or other environmental conditions may change vegetation health and distribution.

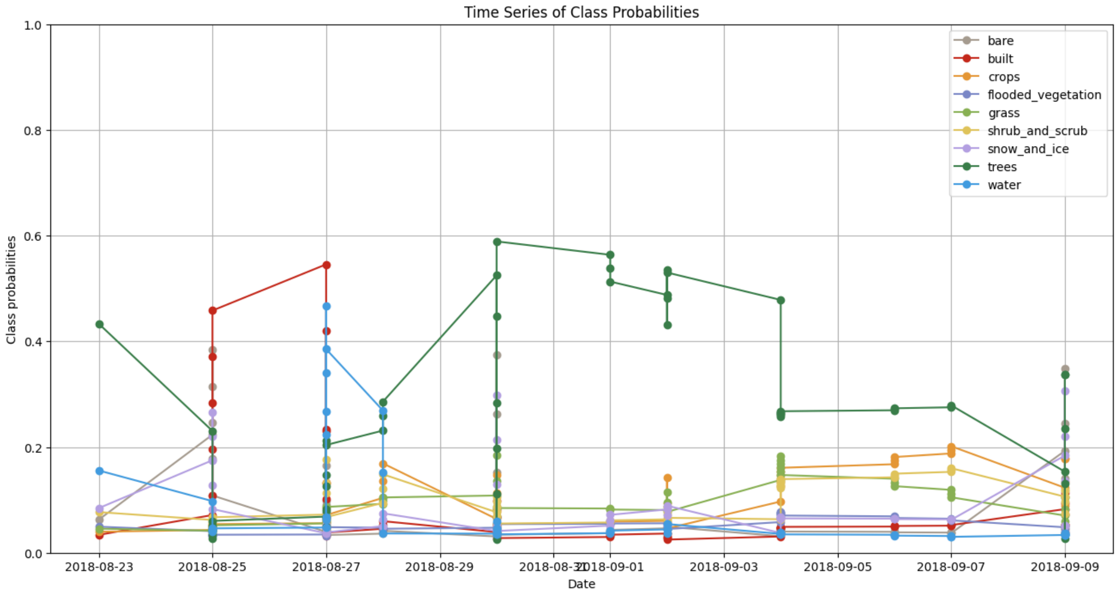

Figure 4.20: Time series of class probability

However, due to the cloud cover brought about by the storm, the changes observed in Figure 4.21 could not be compared to the high-resolution images. Even though we can see changes detected in red (urban areas), these changes are misclassified because of the storm and the clouds. This limitation has narrowed the chance of knowing much more about the changes in land cover. Despite this, through the Internally Displaced People database, we know that about 52,000 individuals have been displaced since then due to the expansion of the water body. This displacement corresponds to the huge peaks of the probability of the water class at that place, indicating significant water-related activity in the area.

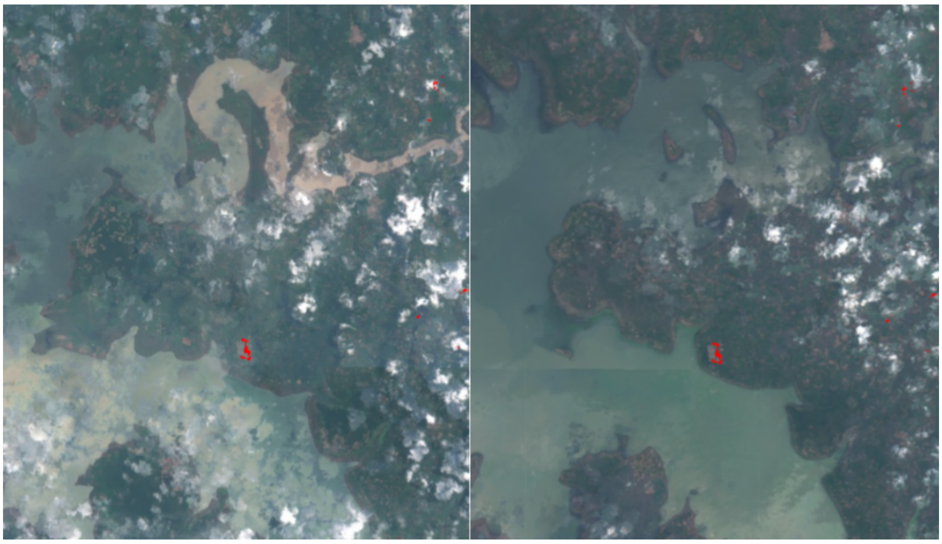

Figure 4.21: Satellite images showing before and after the climate disaster (flood) in Ghana 2018

4.3.2 Study case 2: Nigeria 2018

In Figure 4.22. On the left we shows a composite view of various land cover types across Ghana. Different colors represent different types of land cover. On the right, it focuses specifically on built-up areas extracted from the Dynamic World dataset. The built-up areas are highlighted in white, clearly showing urban and developed regions within the country.

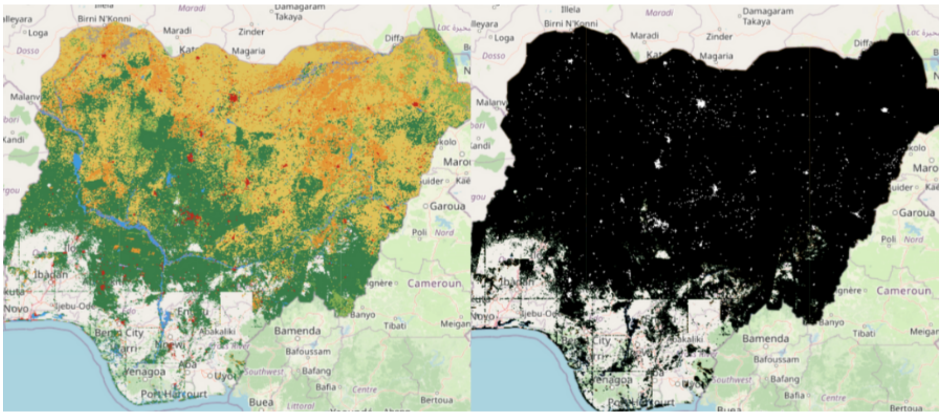

Figure 4.22: Dynamic World Composite and extracted built area image, Nigeria 2018 Brown et al. (2022)

Figure **??** presents the time series of class probabilities for different land cover classes between September 11, 2018, and September 23, 2018. The dates vary along the x-axis, while class probabilities between 0 and 1 are given along the y-axis. Different land cover classes are also distinguished with varying colors, as shown in the legend.

The probability of the class "Trees" proves to be highly variable over the given period. There are distinct peaks around September 13, 17, and 21. These probabilities attain a value of up to 0.6. This shows that there is significant variation in tree cover, maybe due to the different conditions of observation or seasonal changes affecting the vegetation.

The probability for "crops" is more or less consistent throughout the period, though with slight increases corresponding to the peaks seen in the graph for tree cover; the appearance is that agricultural land was constantly present, but with some variation, probably due to agricultural activity or crop condition.

Grassland and shrub/scrub areas are far more constant over time, with the corresponding probabilities ranging from 0.2 to 0.3. This shows that within the period of observation, these land cover types mostly remain the same; therefore, changes in grassland and shrub/scrub areas are pretty low.

In fact, the probabilities for "flooded vegetation" and "water" are pretty low. However, there are some increases towards the exact dates of the high likelihood of tree cover: September 15th and 19th, which could be indicative of temporary flood or, at least, a rise in the water level on these dates.

Most of the observed period indicates that the probability of areas being classified as "urban or built" is low. However, September 15, 2018, there was new urban areas with a peak in the likelihood. This probably means there was a temporary increase in the classification of urban land areas on this date. This peak, therefore, could relate to either changing observatory conditions, anomalies, or even actual developments in the captured urbanized landscape of the remote sensing data.

Other land cover classes, such as "bare, and "snow and ice," maintain low probabilities for the entire duration of the study. This indicates that either these types of land cover are not relevant within the area viewed or that the likelihood of being classified into one of them stays extremely low, which would imply very stable conditions for these types of land.

In conclusion, the Figure 4.23 shows dynamic changes in land cover types over different days, with significant variation in the probabilities of trees and crops. The data indicates possible flooding events, an increase in built areas, and more stable conditions for grassland and shrub/scrub areas. The impact of the flood starting on September 20 is also evident in the observed changes.

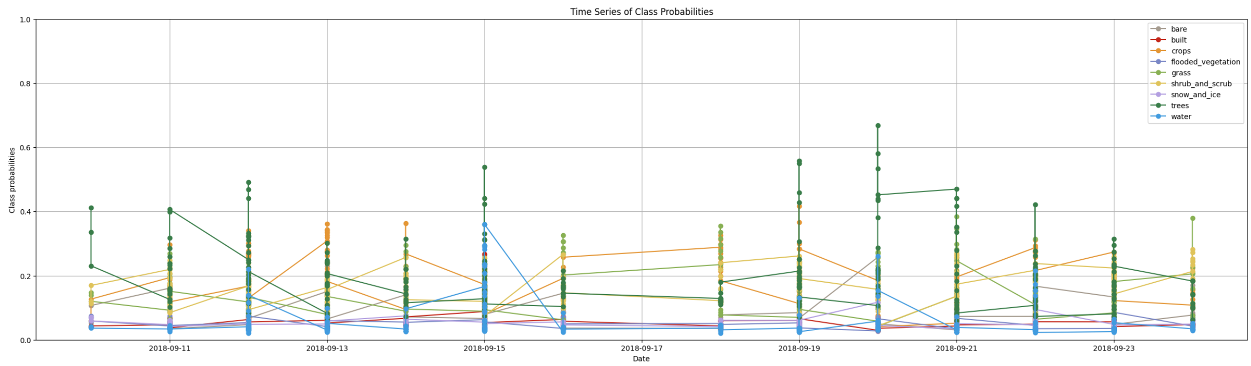

Figure 4.23: Time series of class probability, Nigeria 2018

Now we validate the result by showing before and after disaster in the buffer area using Sentinel-2 a high resolution satellite images. even though there are some areas covered with the cloud, we found new areas and we were able to compare before and after disaster.

Figure 4.24: New urban areas in red, After disaster and before disaster in Nigeria

5. Discussion

This research, therefore, sought to tell the population displacements due to climate-related disasters in Africa between 2000 and 2018 using satellite remote sensing imagery. In integrating high-resolution satellite images with datasets of Landscan population counts Tellman et al. (2021), EM-DAT Centre for Research on the Epidemiology of Disasters (CRED) (2024), and GDIS Rosvold and Buhaug (2021a,b), among others, we tried to link these climate disasters to population movements. This was in line with the short-term and long-term trends of human displacement due to floods, storms, droughts, and heatwaves revealed by the analysis; GIS techniques and change detection models validate the population shifts noted.

The results show a relationship between climate-induced disasters and population dynamics. In Niger, for example, from the case study of the 2011 floods, it was shown that there is a clear trend of population decline in the flooded areas and an increase in the neighboring regions. This would seem to mean that floods led to mass movements of individuals to safer regions. In Ghana, the 2018 floods led to more water bodies and displaced about 52,000 people, as verified by the IDMC database (IDMC).

Comparing all these results with previous research majorly, our findings align with the conclusions made by Wang et al. (2020), who noted that climate conditions change habitability and forced migration. Our research offers specific insights into displacement patterns in the African region and how the movement of people adjusts or becomes dynamic with time.

Theoretically, the research moves forward our understanding of climate-induced migration. We think that our study does show some promise in integrating remote sensing data with traditional disaster data sets to analyze human displacement, work that can be potentially replicated in other regions with other disaster types to make more significant contributions towards more comprehensive models of mobility in response to environmental stressors.

In terms of practical implications, this will significantly affect disaster response and management. With knowledge of population movement at a detailed spatial and temporal scale, policymakers and humanitarian organizations can better plan and allocate resources. For example, knowledge of where displaced people will be hosted can help pre-positioning supplies or even planning evacuation routes.

5.1 Limitations

While this paper shows quite valuable findings, it is not free of limitations. Mainly, the total dependence on satellite imagery is plagued by the problem of cloud cover and other atmospheric disturbances that may create some gaps in data. Secondly, integrating several datasets, each with its inaccuracies, may bring errors to its analysis. For instance, the EM-DAT dataset Centre for Research on the Epidemiology of Disasters (CRED) (2024) does not include very detailed spatial information, for which we used data from GDIS Rosvold and Buhaug (2021a,b); this process of merging the datasets may produce discrepancies.

Also, the time of study may miss the latest trend in climate-induced migration, as climate change is causing more frequent and intense disasters nowadays. Finally, though we used relatively GIS techniques, only a coarse resolution of population data may not be able to capture micro-level movements within urban areas.

Although remote sensing technology offers beneficial insight into climate-induced population movements

, associated ethical concerns have to be responsibly addressed. Much detail can be captured from high resolution imagery about individuals and communities, which raises privacy concerns. As opposed to traditional data collection, people can't give their consent in remote sensing, and this may be ethically less than desirable when sensitive information is being collected. The security of remote sensing data becomes essential. This prevents abuse, particularly where the data reveals the location of internally displaced people. There is, therefore, the need to control open access in consideration of transparency and the possibility of data abuse.

5.2 Ethical concerns

Data from remote sensing is also limited in regions with high cloud frequency, which is again represented in the accuracy and fairness of analyses. This can be limited by using multi-sourced data, along with corresponding data processing methods. For instance, researchers need to consider issues of potential impact on populations, such as risk of targeted violence or exploitation, while upholding ethical norms that safeguard vulnerable groups (United Nations Office for the Coordination of Humanitarian Affairs (OCHA), 2013).

Data collection, analysis, and reporting must be conducted transparently to maintain trust and accountability. Wherever possible, such methodologies and limitations have to be communicated with their implications (Kuffer et al., 2016). The engagement of local communities and stakeholders will ensure respect for the data applied in research (United Nations Office for the Coordination of Humanitarian Affairs (OCHA), 2013).

Aggregation and anonymity do not allow the invasion of private life since the possibility of direct consent will not be possible in collecting remote sensing data. Procedures to control access and constant security will prevent unauthorized access and misuse of secure storage (Bolten et al., 2020). The incidence of the data's ethical implications is always prevented if strict data governance is present (United Nations Office for the Coordination of Humanitarian Affairs (OCHA), 2013). Reducing the bias that is produced through advanced processing techniques along with the integration of many sources provides accuracy and fairness but not at the stake of giving representation to under-represented areas (Mahmood et al., 2010). Ethical guidelines on the use of data should not bring about harm to others, and broader implications could be pondered on by researchers, as well as policymakers. This ensures accountability and instills confidence. The potential of remote sensing is, therefore, realizable ethically when proper standards are followed, together with solid protocols for handling data.

5.3 Future research

Future research should focus on several specific parts to advance the knowledge in this field. It could be done; first, with greater accuracy, by using very high-resolution Imagery, and then more detailed population data to detect the most precise way of capturing and analyzing population movements in response to climate disasters. Secondly, long-term studies on population distribution over time after a climate disaster will help provide insight into the long-term effect and sustainability of post-disaster recovery from the event. Finally, machine learning and deep learning help in obtaining more accurate data that can overcome limitations whereby we are able to have better accuracy in our analysis.

In so doing, we can add to this knowledge that has been established through this study toward more effective responses to what is going to be a growing challenge: that of climate-induced migration.

6. Code availability

Code for the analysis and make all maps is publicly available https://github.com/0xpix/CERI-Project

7. Conclusion

By analyzing high-resolution satellite images and using other incorporation like the Landscan population counts, we have, in some cases we managed to link climate catastrophes and movements of the populations after the disasters in Africa from 2000 to 2018. Still, the data missing from that continent or even the unprecise data did not help much to come to a better conclusion.

In this respect, the present research has furnished the problem with solutions as mentioned above through applying the latest Geographic Information Systems techniques of change detection models and measurement of land cover change in validating population shifts. The monthly and annual analyses have provided an understanding of the short-term and long-term trends relevant to human displacement. These provide a significant knowledge of areas relating to climate-induced migration, especially in Africa. The combination of EM-DAT and GDIS datasets, as well as RSIF data from Copernicus Climate Data, Dynamic World, and other sources, allowed us to conduct a very detailed analysis of population dynamics before and after disaster events.

As such, this study will be essential not only in adding to scientific knowledge but also in providing much-needed information that is going to be fundamental in making practical tools and strategies that deal with issues that are generated by the impact and migration caused by climate change. This study's conclusion would help guide policy framers and various stakeholders to develop more resilient communities and better preparedness for future climate disasters.

Acknowledgements

Firstly, I would like to thank Allah for keeping me thus far and giving me the strength to conquer every challenged I faced with this research when I was on the verge of giving up. I want to acknowledge AIMS and it's funders for supporting this work. I extend my sincere gratitude to Graeme Dor for helping me, and my supervisor Dr.Houriiyah From CERI/Stellenbosch University, thank you for your guidance and invaluable assistance.

Lastly, I would like to thank my family for supporting me: my mom, my dad, all my sisters, my friends and my cousin Hachem.

I want to dedicate a special thank you to my best friend, Masego, for being there for me.

References

Bernzen, A., Jenkins, J. C., and Braun, B. Climate change-induced migration in coastal bangladesh? a critical assessment of migration drivers in rural households under economic and environmental stress. *Geosciences*, 9(1):51, 2019. doi: 10.3390/geosciences9010051.

Bilsborrow, R. E., Hugo, G., Oberai, A., and Zlotnik, H. *International migration statistics: Guidelines for improving data collection systems*. International Labour Office, 1997.

Bircan, T. Remote sensing data for migration research. In *Data Science for Migration and Mobility*, pages 115–140. British Academy, 2022. doi: 10.5871/bacad/9780197267103.003.0006. URL https://doi.org/10.5871/bacad/9780197267103.003.0006.

Blumenstock, J. Inferring patterns of internal migration from mobile phone call records: evidence from rwanda. *Information Technology for Development*, 18:107–125, 04 2012a. doi: 10.1080/02681102.2011.643209.

Blumenstock, J. E. Inferring patterns of internal migration from mobile phone call records: Evidence from rwanda. *Information Technology for Development*, 18(2):107–125, 2012b.

Bolten, J. D., Entekhabi, D., and Njoku, E. G. Remote sensing for agriculture, ecosystems, and hydrology: Ethical considerations and best practices. *IEEE Geoscience and Remote Sensing Magazine*, 8(1):1–19, 2020.

Bright, E., Coleman, P., King, A., and Rose, A. Landscan global 2007, 2008. URL https://doi.org/10.48690/1524203.

Bright, E., Coleman, P., Rose, A., and Urban, M. Landscan global 2009, 2010. URL https://doi.org/10.48690/1524205.

Brown, C. F., Brumby, S. P., Guzder-Williams, B., et al. Dynamic world, near real-time global 10 m land use land cover mapping. *Scientific Data*, 9:251, 2022. doi: 10.1038/s41597-022-01307-4.

Centre for Research on the Epidemiology of Disasters (CRED). Em-dat: The emergency events database, 2024. URL https://www.emdat.be/. Accessed: DAY MONTH YEAR.

Chen, X. Nighttime lights and population migration: Revisiting classic demographic perspectives with an analysis of recent european data. *Remote Sensing*, 12(1), 2020. ISSN 2072-4292. doi: 10.3390/rs12010169. URL https://www.mdpi.com/2072-4292/12/1/169.

Climate, P. Measuring the effect of climate change on migration flows: Limitations of existing data and analytical frameworks. *PLOS Climate*, 10:1–12, 2020. doi: 10.1371/journal.pclm.000001.

Craggs, W. A. Worldwide health risks related to climate change are on the rise. Technical report, World Health Organization, 2023. URL https://www.who.int/news-room/fact-sheets/detail/climate-change-and-health.

Europe, P. How do environmental factors influence migration? *Population Europe*, 10:1–12, 2020. doi: 10.1007/s12303-020-00123-x.

Fang, G., Zhao, L., Cao, S., Zhu, L., and Ge, Y. Estimation of tropical cyclone wind hazards in coastal regions of china. *Natural Hazards and Earth System Sciences*, 20(6):1617–1637, 2020. doi: 10.5194/nhess-20-1617-2020. URL https://nhess.copernicus.org/articles/20/1617/2020/.

Fang, Z. L. C. S. Z. L. . G. Y., G. Estimation of tropical cyclone wind hazards in coastal regions of china. *Natural Hazards and Earth System Sciences*, 20:1617–1637, 2020. doi: 10.5194/nhess-20-1617-2020.

Google Earth Engine. Image collection reducers. https://developers.google.com/earth-engine/guides/reducers_image_collection, 2024a. Accessed: DAY MONTH YEAR.

Google Earth Engine. Introduction to dynamic world - part 3. https://developers.google.com/earth-engine/tutorials/community/introduction-to-dynamic-world-pt-3, 2024b. Accessed: DAY MONTH YEAR.

Gorelick, N., Hancher, M., Dixon, M., Ilyushchenko, S., Thau, D., and Moore, R. Google earth engine: Planetary-scale geospatial analysis for everyone. *Remote Sensing of Environment*, 202:18–27, 2017. doi: 10.1016/j.rse.2017.06.031. URL https://doi.org/10.1016/j.rse.2017.06.031.

Health, B. P. Tracking the impacts of climate change on human health via indicators: lessons from the lancet countdown. *BMC Public Health*, 20:1–15, 2020. doi: 10.1186/s12889-020-09387-y.

Hoffmann, R., Dimitrova, A., Muttarak, R., Crespo Cuaresma, J., and Peisker, J. A meta-analysis of country-level studies on environmental change and migration. *Nature Climate Change*, 10:904–912, 2020. doi: 10.1038/s41558-020-0898-6. URL https://doi.org/10.1038/s41558-020-0898-6.

Hugo, G. Improving statistics on international migration in asia. *International Statistical Review*, 74(3): 335–355, 2006.

(IDMC), I. D. M. C. Global internal displacement database. https://www.internal-displacement.org/database, 2024. Accessed: 2024-06-15.

Joyce, K. E., Belliss, S. E., Samsonov, S. V., McNeill, S., and Glassey, P. J. A review of the status of satellite remote sensing and image processing techniques for mapping and monitoring natural hazards. *Progress in Physical Geography*, 33(2):183–207, 2009. doi: 10.1177/0309133309339563.

Karantanellis, E. et al. Satellite imagery for rapid detection of liquefaction surface manifestations: The case study of türkiye–syria 2023 earthquakes. *Remote Sensing*, 15(17):4190, 2023.

Knutson, T. R., McBride, J. L., Chan, J., Emanuel, K., Holland, G., Landsea, C., Held, I., Kossin, J. P., Srivastava, A. K., and Sugi, M. Tropical cyclones and climate change. *Nature Geoscience*, 3 (3):157–163, 2010. doi: 10.1038/ngeo779.

Kuffer, M., Pfeffer, K., and Sliuzas, R. Slums from space—15 years of slum mapping using remote sensing. *Remote Sensing*, 8(6):455, 2016.

Liu, L., Zhang, X., and Zhao, T. Glc fcs30d: the first global 30 m land-cover dynamic monitoring product with fine classification system from 1985 to 2022, 2023. URL https://doi.org/10.5281/zenodo.8239305.

Mahmood, R., Pielke, R. A., and Hubbard, K. G. Impacts of land use/land cover change on climate and future research priorities. *Bulletin of the American Meteorological Society*, 91(1):37–46, 2010.

Mbaye, L. and Okara, A. Climate change, natural disasters, and migration. *IZA World of Labor*, (346), 2023. doi: 10.15185/izawol.346.v2.

Ofori, D. O., Bandauko, E., Kutor, S. K., Odoi, A., Asare, A. B., Akyea, T., and Arku, G. A systematic review of international and internal climate-induced migration in africa. *Sustainability*, 15(22), 2023. ISSN 2071-1050. doi: 10.3390/su152216105. URL https://www.mdpi.com/2071-1050/15/22/16105.

Piguet, E., Pecoud, A., and de Guchteneire, P. *Climate and Human Migration: Past Experiences, Future Challenges*. Cambridge University Press, 2011.

Ritchie, H. and Rosado, P. Natural disasters. *Our World in Data*, 2022. https://ourworldindata.org/natural-disasters.

Rosvold, E. and Buhaug, H. Geocoded disasters (gdis) dataset, 2021a. URL https://doi.org/10.7927/zz3b-8y61. Accessed DAY MONTH YEAR.

Rosvold, E. L. and Buhaug, H. Gdis, a global dataset of geocoded disaster locations. *Scientific Data*, 8:61, 2021b. doi: 10.1038/s41597-021-00846-6.

Roy, S. and Swetnam, T. samapriya/awesome-gee-community-datasets: Community catalog (2.6.0), 2024. URL https://doi.org/10.5281/zenodo.11118613.

Shaw, N. T. and McGuire, S. K. Understanding the use of geographical information systems (giss) in health informatics research: a review. *BMJ Health & Care Informatics*, 24(2):228–233, 2017. doi: 10.14236/jhi.v24i2.940. URL https://informatics.bmj.com/content/24/2/228.

Silva-Coira, F., Paramá, J. R., Ladra, S., López, J. R., and Gutiérrez, G. Efficient processing of raster and vector data. *PLOS ONE*, 15(1):e0226943, 2020. doi: 10.1371/journal.pone.0226943. URL https://doi.org/10.1371/journal.pone.0226943.

Singh, A. et al. Assessing river bank erosion in the ganges using remote sensing and gis. *Environmental Monitoring and Assessment*, 195(2):245, 2023.

Tellman, B., Sullivan, J. A., Kuhn, C., Kettner, A. J., Doyle, C. S., Brakenridge, G. R., Erickson, T., and Slayback, D. A. Satellites observe increasing proportion of population exposed to floods. *Nature*, 2021. doi: 10.1038/s41586-021-03695-w. Accepted.

Thomas, V. and López, R. Global increase in climate-related disasters. Technical report, Asian Development Bank, 2015. URL http://hdl.handle.net/11540/5274.

Turner, B. L., Meyer, W. B., and Skole, D. L. *People and pixels: Linking remote sensing and social science*. National Academy Press, 1995.

United Nations Office for the Coordination of Humanitarian Affairs (OCHA). *Ethical Considerations for Remote Sensing and Data Collection in Humanitarian Work*. Number 014 in OCHA Policy and Studies Series. 2013.

Vatsavai, R. et al. Rapid damage assessment using high-resolution remote sensing imagery: Tools and techniques. In *2011 IEEE International Geoscience and Remote Sensing Symposium*, pages 1445–1448, Vancouver, BC, Canada, July 2011. IEEE. doi: 10.1109/IGARSS.2011.6049338. URL https://doi.org/10.1109/IGARSS.2011.6049338.

Venter, Z. S., Barton, D. N., Chakraborty, T., Simensen, T., and Singh, G. Global 10 m land use land cover datasets: A comparison of dynamic world, world cover and esri land cover. *Remote Sensing*, 14 (16), 2022. ISSN 2072-4292. doi: 10.3390/rs14164101. URL https://www.mdpi.com/2072-4292/14/16/4101.

Voigt, S., Kemper, T., Riedlinger, T., Kiefl, R., Scholte, K., and Mehl, H. Global trends in satellite-based emergency mapping. *Science*, 353(6296):247–252, 2016.

Walls, M. A., Pesek, S., and Peterson, D. Flooding in the united states 101: Causes, trends, and impacts, 2023. Accessed: 2024-06-15.

Wang, M., Challis, R., and Lacey, M. Masst: A tool for reuse of public ms data. *Journal of Metabolomics*, 16(2):167–176, 2020.

Wu, Q. Geemap: A python package for interactive mapping with google earth engine. *Journal of Open Source Software*, 5(51):2305, 2020. doi: 10.21105/joss.02305. URL https://doi.org/10.21105/joss.02305.

Xu, Q. and Freitas, M. A. Massmatrix: A tandem mass spectrometry database search tool. *Journal of Proteomics*, 8(9):1576–1588, 2009.

Zagheni, E., Weber, I., and Gummadi, K. P. Leveraging facebook's advertising platform to monitor stocks of migrants. *Population and Development Review*, 40(4):721–734, 2014.

Zhang, C., Li, Z., and Bowers, K. Eo-based ex post assessment of idp camp evolution and population dynamics in zam zam, darfur. *Remote Sensing*, 11(1):75–89, 2019.